ATAXIA

Reduced cerebellar rhythm by climbing fiber denervation is linked to motor rhythm deficits in mice and ataxia severity in patients

Chih-Chun Lin[1,2,3,4]†, Ke-Chu Fang[5,6]†, Ilaria Balbo[3,4]†, Ting-Yu Liang[5,6,7], Chia-Wei Liu[5,6], Wen-Chuan Liu[5,6,7], Yi-Mei Wang[8], Yen-Ling Hung[5], Kai-Chien Yang[5], Scott Kun Geng[9], Chun-Lun Ni[3,4,10], Christopher P. Driscoll[3,4], David S. Ruff[3,4], Ami Kumar[3,4], Nadia Amokrane[3,4], Natasha Desai[3,4], Phyllis L. Faust[11], Elan D. Louis[12], Sheng-Han Kuo[3,4]*, Ming-Kai Pan[5,6,7,8,13,14]*

Cerebellar ataxia results from various genetic and nongenetic disorders and is characterized by involuntary movements that impair precision and motor rhythm. Here, we report that climbing fiber (CF) denervation is a common pathophysiology underlying motor rhythm loss in cerebellar ataxia. By examining cerebellar pathology in patients with spinocerebellar ataxia (SCA) types 1, 2, and 6 and multiple system atrophy, we identified CF degeneration with synaptic loss as a shared pathophysiology. Optogenetic silencing of CF synaptic activity in mice induced ataxia-like motor dysfunctions and loss of motor precision. In addition, CF silencing resulted in cerebellar and motor rhythm loss, another core feature of ataxia. This rhythm loss was predominantly CF dependent and resistant to Purkinje cell–specific lesioning by diphtheria toxin. Correspondingly, two patients with inferior olive pathology, the brain site that provides CFs to Purkinje cells, presented with ataxia and cerebellar rhythm loss. Patients with genetic or nongenetic cerebellar ataxia exhibited cerebellar rhythm loss that correlated with the Scale for the Assessment and Rating of Ataxia. Chemogenetic stimulation of CFs improved cerebellar and motor rhythms as well as motor performance in the SCA type 1 mouse model of ataxia. These results suggest that CF-dependent cerebellar rhythm loss occurs across different types of cerebellar ataxia, contributing to motor imprecision and motor rhythm loss, two defining features of ataxia.

INTRODUCTION

Ataxia is defined as a lack of movement coordination associated with loss of motor rhythm (dysrhythmia). It consists of disabling clinical symptoms of imbalance, frequent falls, and loss of fine motor control. These symptoms can arise from various genetic and nongenetic causes of cerebellar dysfunction (*1*, *2*). Although gene therapies and other treatments aim at slowing or halting the progression of cerebellar ataxia, they do not address the immediate ataxia symptoms that patients experience (*3*). In addition, a large portion of patients with cerebellar ataxia do not have identifiable genetic causes, posing challenges to therapeutic development in this population. Therefore, identifying and targeting the common brain circuit alterations in cerebellar ataxia could potentially yield circuit-based therapies to alleviate symptoms.

[1]Ataxia Center, Department of Neurology, Massachusetts General Hospital, Boston, MA 02114, USA. [2]Department of Neurobiology, Harvard Medical School, Boston, MA 02115, USA. [3]Department of Neurology, College of Physicians and Surgeons, Columbia University, New York, NY 10032, USA. [4]Initiative for Columbia Ataxia and Tremor, Columbia University, New York, NY 10032, USA. [5]Department and Graduate Institute of Pharmacology, National Taiwan University College of Medicine, Taipei 10051, Taiwan. [6]Molecular Imaging Center, National Taiwan University, Taipei 106038, Taiwan. [7]Department of Medical Research, National Taiwan University Hospital, Taipei 10002, Taiwan. [8]Cerebellar Research Center, National Taiwan University Hospital, Yun-Lin Branch, Yun-Lin 64041, Taiwan. [9]Department of Computer Science, Columbia University, New York, NY 10027, USA. [10]Department of Biochemistry and Molecular Biology, Indiana University School of Medicine, Indianapolis, IN 46202, USA. [11]Department of Pathology and Cell Biology, College of Physicians and Surgeons, Columbia University, New York, NY 10032, USA. [12]Department of Neurology, University of Texas Southwestern Medical Center, Dallas, TX 75390, USA. [13]Institute of Biomedical Sciences, Academia Sinica, Taipei 11529, Taiwan. [14]Research Center for Developmental Biology and Regenerative Medicine, National Taiwan University, Taipei 10638, Taiwan.
*Corresponding author. Email: sk3295@columbia.edu (S.-H.K.); emorymkpan@ntu.edu.tw (M.-K.P.)
†These authors contributed equally to this work.

Studies in animal models of cerebellar ataxia have delineated the process of Purkinje cell (PC) degeneration. Initially, PCs lose their excitatory synapses, including climbing fiber (CF)–to-PC synapses, followed by subsequent PC death in various genetic models of cerebellar ataxias (*4*–*6*). However, it remains unclear whether CF synaptic loss occurs in human cerebellar ataxic disorders and how this loss of synaptic activity contributes to the loss of motor rhythm and precision. This gap in understanding represents an important bottleneck for developing synaptic interventions and therapies.

The overarching aim of this study was to investigate the potential roles of CFs in ataxia pathophysiology. Specifically, we aimed to study the impact of CF loss in dysrhythmia, which separates it from other cerebellar dysfunctions like essential tremor, a gain of rhythm disorder with excessive olivocerebellar oscillations (*7*, *8*). We found CF synaptic loss in postmortem human brains of donors with cerebellar ataxia and showed that reduced cerebellar rhythm correlated with the severity of clinical symptoms. Inhibition of CF synapses disrupted cerebellar rhythm and induced ataxia-like behavior in wild-type (WT) mice, whereas CF stimulation could improve cerebellar rhythm and motor function in an ataxia mouse model. Our study indicates that CF synaptic loss and reduced cerebellar rhythm are common pathological features of cerebellar ataxia, suggesting CF stimulation as a potential therapeutic target.

RESULTS

CF synaptic retraction is a shared pathological feature in cerebellar ataxia

We first examined the postmortem human cerebellar tissue from controls and patients with cerebellar ataxia including spinocerebellar ataxia (SCA) types 1, 2, and 6 and the cerebellar type of multiple system

atrophy (MSA-C) (table S1). We found that ~60% of PCs were gone in the brains of patients with cerebellar ataxia (41.5% remaining PCs in patients with cerebellar ataxia compared with those in controls; table S1). However, the remaining PCs in patients were not entirely normal but showed lower CF synaptic density (Fig. 1, A to F, control versus cerebellar ataxia: 21.2 ± 1.1 versus 15.0 ± 4.7 puncta/100 μm, $P < 0.001$; please refer to data file S1 for all data points, quantitative statistic results, and effect sizes in this and the following figures). We next examined the distribution of CF synapses in the postmortem cerebellum. Normally, CFs arise from the inner part of the molecular layer and extend distally to the outer part to form CF synapses (*9*, *10*). However, when we examined the outer 20% portion of the molecular layer, patients with cerebellar ataxia showed CF synaptic regression (Fig. 1G, control versus cerebellar ataxia: 22.3 ± 2.9% versus 11.3 ± 5.8, $P < 0.001$).

Only a small proportion of CFs reaches the outer 20% of the molecular layer in healthy individuals, making the outer 20% measurement more suitable to describe CF overgrowth (as seen in essential tremor) than CF loss. To faithfully reveal the CF retraction in patients with ataxia, we also calculated the synaptic density in the outer 50% of molecular layers and again found reduced percentages of CF synaptic puncta (Fig. 1H, controls versus cerebellar ataxia: 89.1 ± 4.9% versus 70.3 ± 14.1%, $P < 0.001$). To investigate whether age and gender contribute to the pathological changes described above (CF density, CFs at outer 20% of the molecular layer, and CFs at outer 50% of the molecular layer), we performed multivariable linear regression analyses with age, sex, and diagnosis (control or cerebellar ataxia). The differences in the CF distribution at the outer 20 or 50% of the molecular layer between cerebellar ataxia and control remained after adjusting for age and sex (table S2). The CF regression was not correlated with PC loss, suggesting that the CF pathology is not an epiphenomenon reflecting PC density (Fig. 1, I and J). We further investigated whether CF synaptic retraction is a common observation in genetic versus nongenetic causes of cerebellar ataxia and found similar CF synaptic density in both genetic (SCA types 1, 2, and 6) and nongenetic (MSA-C) cerebellar ataxias (fig. S1, A to C).

Silencing CF activity leads to cerebellar ataxia–like motor deficits

To assess the changes in motor function after the loss of CF activity, we acutely suppressed CF activity in WT mice with intact

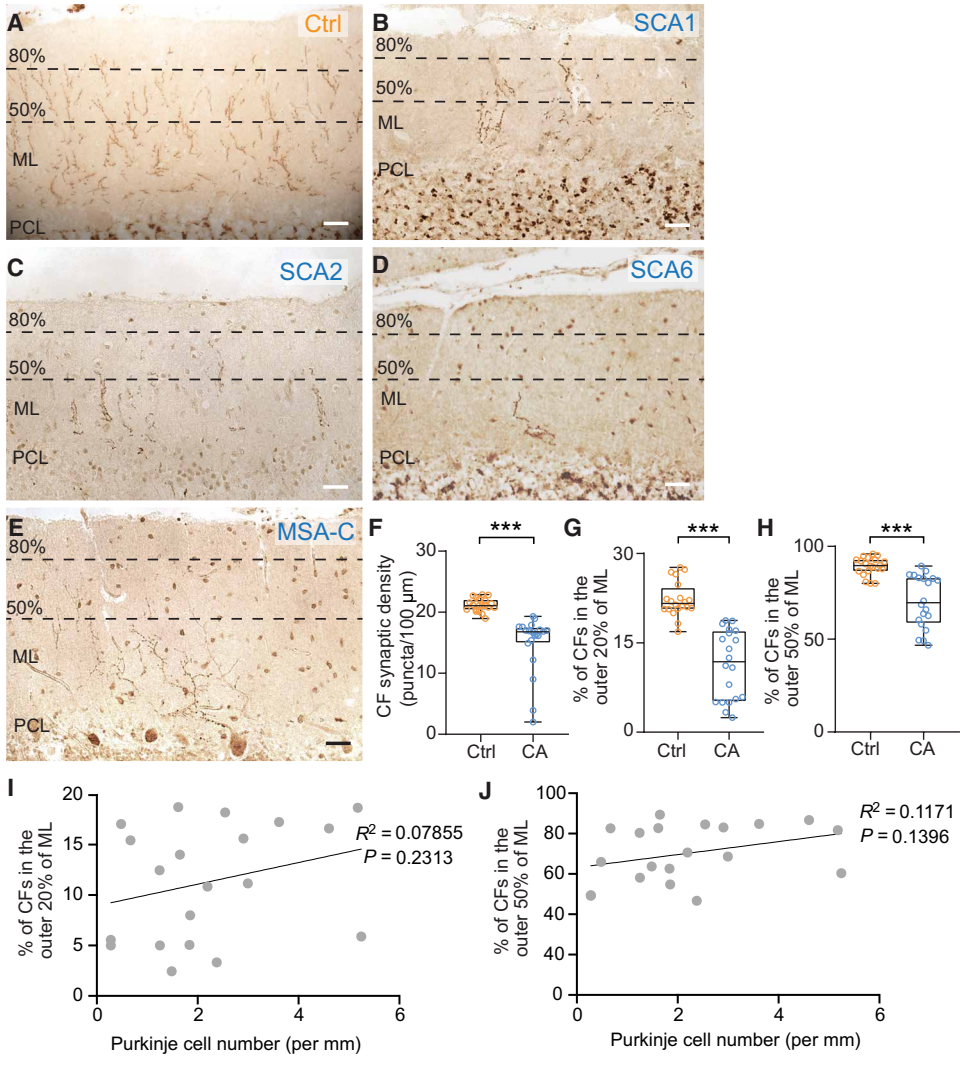

Fig. 1. Pathological features in the cerebella of patients with various causes of cerebellar ataxia. (**A** to **E**) Representative images of vesicular glutamate transporter type 2 (VGlut2) immunohistochemistry visualizing CFs in postmortem parasagittal cerebellar tissue from a control individual (A), a patient with SCA1 (B), SCA2 (C), SCA6 (D), and MSA-C (E). The upper line marks the outer 20% of the molecular layer, and the lower line marks the 50% point of the molecular layer. Scale bars, 50 μm. (**F**) CF synaptic density (puncta/100 μm) in control individuals versus patients. (**G**) Percentages of CFs in the outer 20% of the molecular layer. (**H**) Percentages of VGlut2 CF puncta in the outer 50% of the molecular layer. (**I** and **J**) Correlations between PC density and CF density in outer 20 or 50%, respectively ($n = 20$ control participants and $n = 20$ patients). CA, cerebellar ataxia; Ctrl, control; ML, molecular layer; PCL, Purkinje cell layer. Data are presented with box and whisker plots. ***$P < 0.001$, Student's t test.

cerebellar circuitry. AAV9-CaMKIIa-stGtACR2-FusionRed (*11*) was delivered to the inferior olive (IO), the origin of CFs, to express a light-activated chloride channel under the calcium- and calmodulin-dependent protein kinase IIa (CaMKIIa) promoter (Fig. 2, A and B). We then applied cannula-guided blue light to bilateral IOs and evaluated its impact on ataxia-related motor performance using balance beam tests, video-based gait analysis, and reaching kinematics. Optogenetic IO silencing increased the beam traversal time and the number of slips in mice (Fig. 2, C to E, and movie S1). Video-based gait analysis (Fig. 2, F to I, and movie S2) also revealed a deterioration in gait precision, affecting stride length and its variability (Fig. 2, J to M). Stimulation with nonactivating light did not induce motor deficits, ruling out nonspecific thermal effects (fig. S2, A to J). IO silencing also caused unstable limb trajectories (fig. S3, A to C) during skilled reaching movements (movie S3), as documented by angle analysis along the moving trajectories (fig. S3, D to F) without changing moving speed (fig. S3, G and H).

In theory, optogenetic silencing of IO may also affect intra-IO axons in addition to silencing CF activity. To achieve specific manipulation of CF synaptic activity, we used another optogenetic approach targeting synaptic vesicle release at CF axonal terminals onto PC dendrites. Through intra-IO adeno-associated virus (AAV) transduction, a fusion protein of synaptophysin, mini singlet oxygen generator (miniSOG), and citrine (SYP-miniSOG-citrine) was expressed at CF axonal terminals (fig. S4, A and B). When exposed to blue light (473 nm), miniSOG generates free radicals that destroy adjacent SNARE (soluble *N*-ethylmaleimide–sensitive factor attachment protein receptor) proteins, thereby interfering with synaptic vesicle release (*12*), resulting in CF synaptic inhibition, as validated in our previous work (*8*). Similar to the results of IO silencing, CF synaptic silencing also led to ataxic-like motor deficits and motor imprecision (fig. S4, C to N). Nonactivating light did not alter the motor performance (fig. S5, A to H). Together, the loss of CF activity, whether through IO silencing or disruption of CF synaptic release, led to ataxic-like motor behaviors in mice.

Silencing CF activity disturbs motor rhythm in mice

Video-based gait analysis also allowed us to quantify the temporal precision of coordinated movement between limbs (Fig. 2N). Normal mice had highly coordinated limb movements, but IO silencing disturbed the coordination, documented by reduced phase stability of interlimb motions (Fig. 2, O to Q) that can be quantified by polarity index, a numerical parameter between 0 (purely random) and 1 (completely phase-locked). Similar gait dysfunctions were also observed after miniSOG-based CF synaptic silencing (fig. S4, L to N). The phase instability suggests that there may be unstable rhythm control of motion, the other core feature of ataxia apart from impaired motor precision.

To quantify motor rhythm, we evaluated the frequency spectrum of freely moving mice with a pressure-sensing force plate, which has been validated as a reliable tool for tracking motor kinematics in both normal and tremor mice (*7*, *8*, *13*). The intrinsic oscillatory property (IOP) of the force plate allowed us to calibrate overall motor kinetic energy to peak IOP (fig. S6, A to G) (*13*). We first evaluated the spectral features of freely moving behaviors in WT mice. Consistent with previous studies (*8*, *14*), this open-field behavior exhibited a physiological motor rhythm with a slight elevation of the power spectrum density (PSD) peak around 10 Hz. Next, we investigated the impact of optogenetic IO silencing on motor rhythm (Fig. 3, A and B, and movie S4). IO silencing acutely and reversibly disrupted this 10-Hz peak of innate motor rhythm and caused rhythm loss (Fig. 3, C to F). CF synaptic silencing showed a similar motor rhythm loss (fig. S7, A to F). Nonactivating light on CF (fig. S7G) or IO (fig. S8, A to G) did not affect motor rhythm.

To understand whether the motor rhythm loss also exists in mouse models of ataxia, we evaluated the cerebellar histopathology and motor behaviors in the SCA1[82Q] mouse model that expresses the human *ATXN1* gene with polyglutamine expansion (82Q) (*4*, *15*–*19*). The SCA mice developed modest PC loss and CF retraction in the cerebellum (fig. S9, A to E) and typical behavioral deficits in the balance beam test (fig. S9F). Compared with WT mice, the SCA1 mice showed reduced motor rhythm around 10 Hz (fig. S9, G to L).

In summary, loss of CF activity disturbs motor precision and causes motor rhythm loss, thus generating both core features of ataxic behaviors. SCA1 mice with modest CF retraction also developed similar but less severe rhythm loss.

Silencing of CF activity leads to cerebellar rhythm loss in mice

CFs are known to control the rhythmic firing patterns of PCs (*20*, *21*), and the olivocerebellum plays a central role in tremor-related cerebellar oscillations (*7*, *8*). Therefore, we next measured cerebellar local field potentials (LFPs) to study the effects of CF inhibition on the rhythmicity of cerebellar activity (Fig. 3, G and H). Similar to the motor rhythm, the cerebellar LFPs in WT mice showed a mild increment of oscillatory strength around 10 Hz (Fig. 3I), on top of the roughly 1/frequency (1/*f*) physiological LFP noise due to the populational neuronal activities with Poisson distribution at the background (*22*–*24*). Optogenetic IO silencing reversibly suppressed this 10-Hz LFP feature in the cerebellum (Fig. 3I). The 1/*f* LFP background in the spectral diagram is a decremental shape with higher power at the lower frequencies, which may bias the LFP peak detection to lower frequencies. To make the peak measurement more reliable under the 1/*f* background, we also subtracted the mean of the baseline LFP spectrums (Fig. 3J) from each LFP spectrum (Fig. 3K). Both the raw (Fig. 3, L and M) and adjusted (Fig. 3, N and O) spectral diagrams confirmed that IO silencing suppressed the 10-Hz peak of cerebellar rhythms and reduced overall cerebellar rhythms. To exclude the possibility that cerebellar rhythm loss is an epiphenomenon due to reduced motility in ataxic mice (fig. S10, A to D), we further analyzed the LFPs in moving epochs with matched moving velocities. After calibrating the moving velocities, IO silencing still revealed cerebellar rhythm loss (fig. S10, E to G). Besides IO silencing, CF synaptic silencing also revealed similar effects on LFP suppression (fig. S11, A to G). Consistent with the results of motor rhythm, nonactivating light did not alter the cerebellar oscillatory patterns (S11, H and I).

PC lesioning in the motor cerebellum does not alter motor rhythm

CF retraction and PC loss are shared pathophysiologies across ataxic syndromes. We next investigated whether PC loss can generate similar ataxic-like motor deficits in precision and rhythm. We chose an AAV carrying Cre-inducible constructs generating diphtheria toxin and injected the virus into the cerebellar cortices of *PCP2-cre* mice, a PC-specific reporter line (Fig. 4A). This manipulation led to ~65% of PC-specific lesioning in the motor cerebellum with

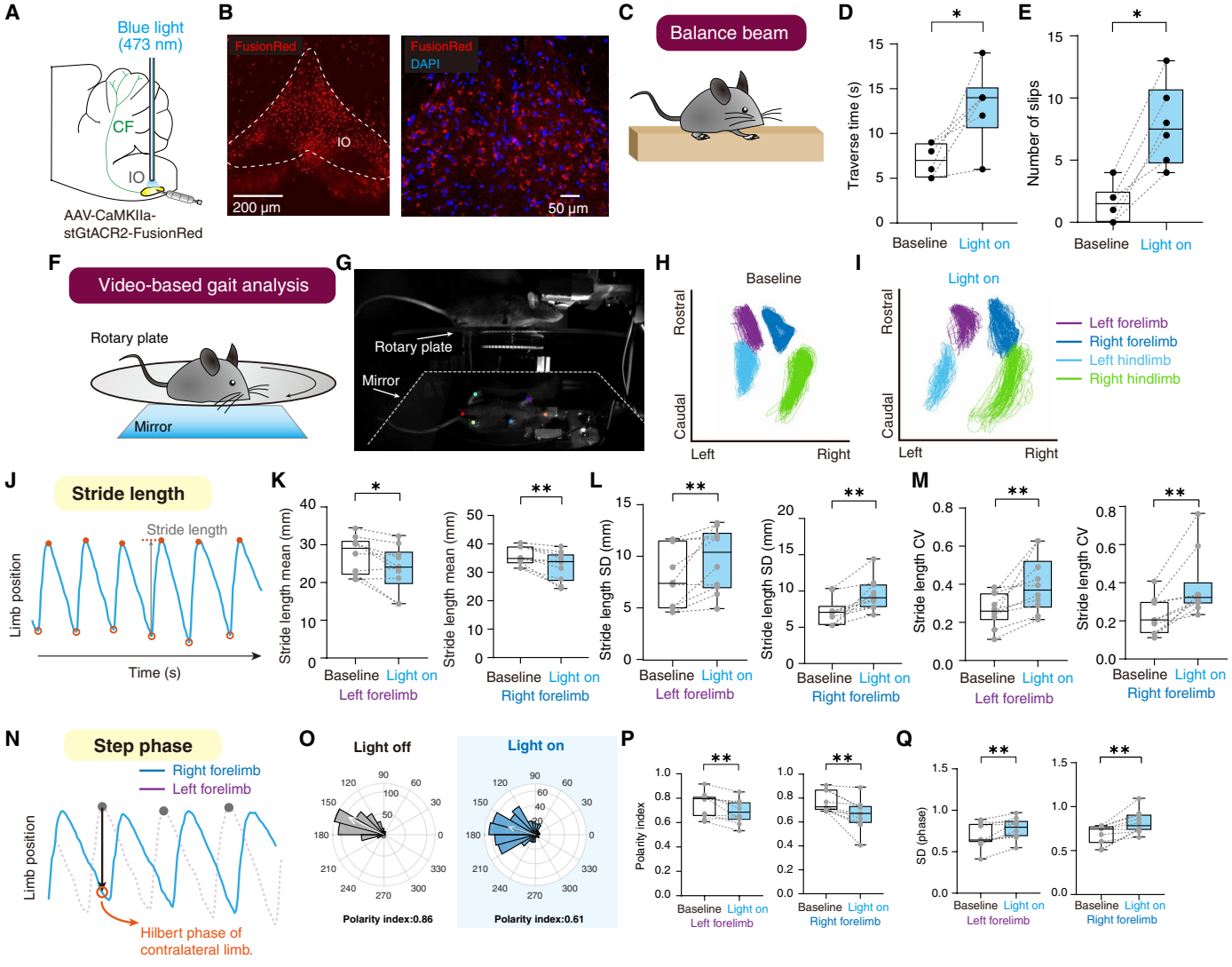

Fig. 2. Silencing of CF activity results in motor deficits similar to cerebellar ataxia in mice. (**A**) Schematic representation of viral transduction with stGtACR2-FusionRed in the IO and subsequent optogenetic silencing. (**B**) Representative images illustrating IO expression of stGtACR2-FusionRed. DAPI, 4′,6-diamidino-2-phenylindole. (**C** to **E**) Motor performance before and during silencing of CF activity in a balance beam test. (C) Quantification of traverse time to cross the beam (D) and the number of foot slips on the beam (E) ($n = 6$ mice). (**F** and **G**) Motor coordination before and during silencing of CF activity was evaluated by video-based gait analysis. (**H** and **I**) Representative limb trajectories before (H) and during (I) optogenetic silencing of the IO. (**J**) Schematic of stride length based on limb position and time. (**K** to **M**) Statistical analysis of the mean stride length (K), SD (L), and coefficient of variation (CV) (M) in the left and right forelimbs, before and during optogenetic stimulation. (**N**) Illustration of the step phases in the right and left forelimbs, calculated using the Hilbert phase of contralateral limb–based motor kinematics. (**O**) Representative polar histograms and polarity indexes of the step phases. (**P** and **Q**) Statistical analysis of the step phase polarity index (P) and SD (Q) on the left and right forelimbs ($n = 10$ mice). Data are presented with box and whisker plots. *$P < 0.05$; **$P < 0.01$, Wilcoxon signed-rank test.

self-produced diphtheria toxin in transfected PCs (Fig. 4, B and C), comparable to PC loss of end-stage patients at autopsy (table S1). Consistent with previous studies (*25*, *26*), PC lesioning led to ataxia-like motor deficits (fig. S12, A to G, and movie S5). In contrast with our prediction, such massive PC loss did not cause motor rhythm loss (Fig. 4, D to H). We further analyzed the cerebellar LFPs in these PC-lesioned mice, which showed cerebellar oscillatory patterns similar to those of control mice (Fig. 4, I to M, and fig. S13, A to G). In contrast with motor precision, which is sensitive to both CF manipulation and PC loss, motor rhythm is predominantly controlled by a CF-dependent mechanism resistant to ~60% of PC loss in mice.

Patients with IO degeneration show cerebellar rhythm loss

Next, we wanted to investigate whether cerebellar rhythm loss can also be observed in patients with cerebellar ataxia. As a proof of principle, we first recorded cerebellar electroencephalography (EEG) (*7*, *8*, *27*) (Fig. 5A) in two patients with IO degeneration and ataxia symptoms (patient 1: 71-year-old male; patient 2: 72-year-old female) with no identifiable pathology from brain magnetic resonance imaging (MRI) except for IO hyperintensity of the T2-weighted images (Fig. 5, B and C). Such a finding suggests prior damage of the IO with subsequent gliosis. As compared with the cerebellar oscillatory features in an age-matched control (72-year-old female) (Fig. 5D), the patients with IO degeneration

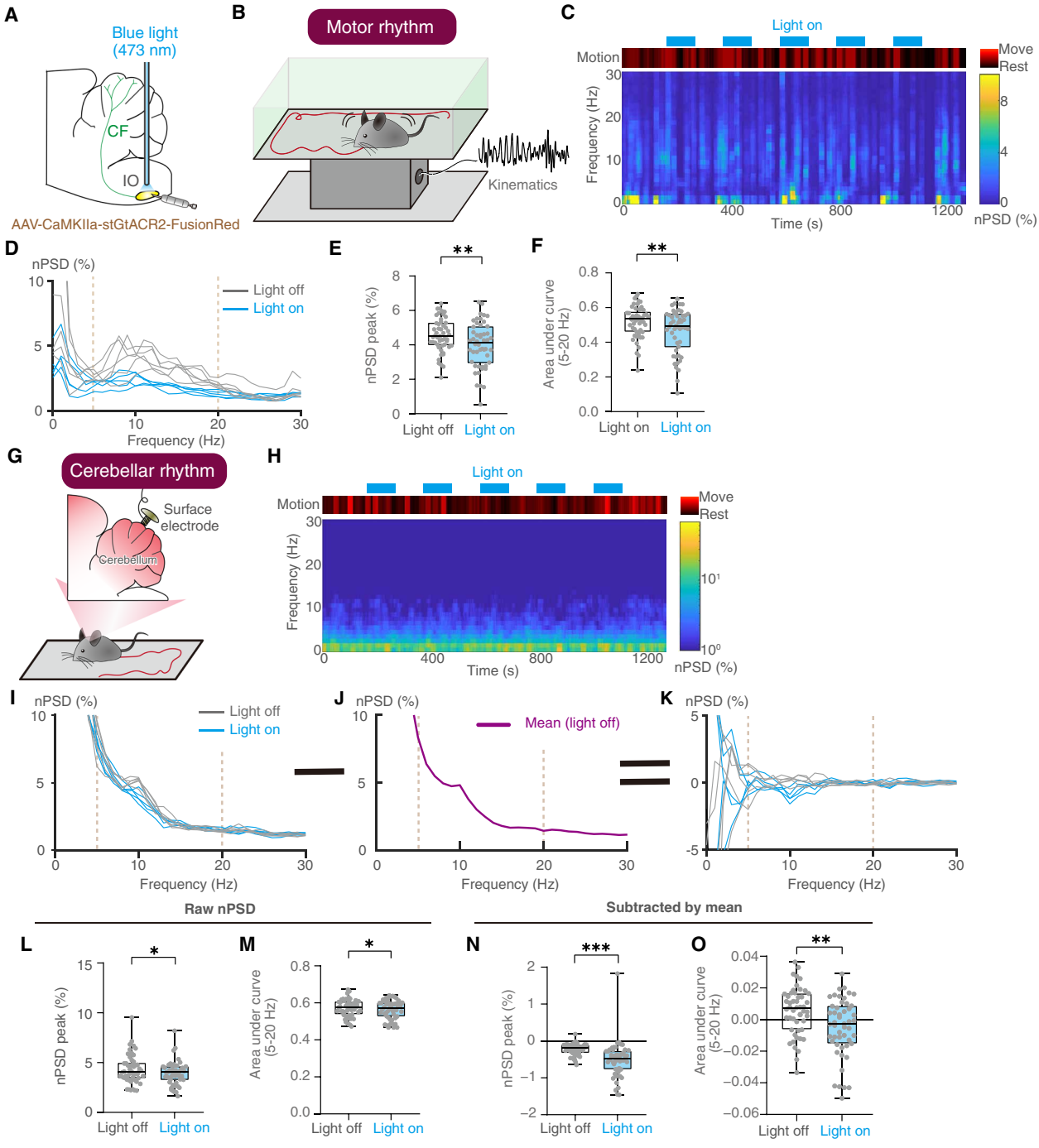

Fig. 3. Optogenetic silencing of the IO results in loss of motor and cerebellar rhythm in mice. (**A**) Schematic representation of viral transduction of stGtACR2-FusionRed in the IO and optogenetic silencing. (**B**) Experimental setup for motor rhythm recordings. (**C**) Detected motion and corresponding time-frequency plot of the recorded motion rhythms during trials of optogenetic manipulation in a representative mouse. Motion was quantified by force plate–based intrinsic oscillations (fig. S6). (**D**) Normalized power spectral diagram (nPSD) of recorded motor rhythms during a sequence of light on and off trials. Each nPSD line was from one trial of (C). (**E** and **F**) Group analysis of the peak nPSDs and the area under the curve of nPSDs between 5 and 20 Hz during light off and on ($n = 10$ mice, five trials per mouse per group). (**G**) Schematic representation of cerebellar LFP recordings in freely moving mice. (**H**) Representative time-frequency plot of cerebellar LFPs and corresponding motion under optogenetic manipulation. (**I**) nPSDs corresponding to individual light-on and -off trials in (H). (**J**) Mean nPSD of light-off trials in (I). (**K**) Mean nPSDs subtracted from nPSDs in (J). (**L** to **O**) Group analysis of nPSD peaks and the area under the curve (5 to 20 Hz) of nPSDs from (J) [(L) and (M)] or (L) [(N) and (O)] ($n = 10$ mice, five sections per mouse per group). Data are presented with box and whisker plots. *$P < 0.05$; **$P < 0.01$; ***$P < 0.001$, Wilcoxon signed-rank test.

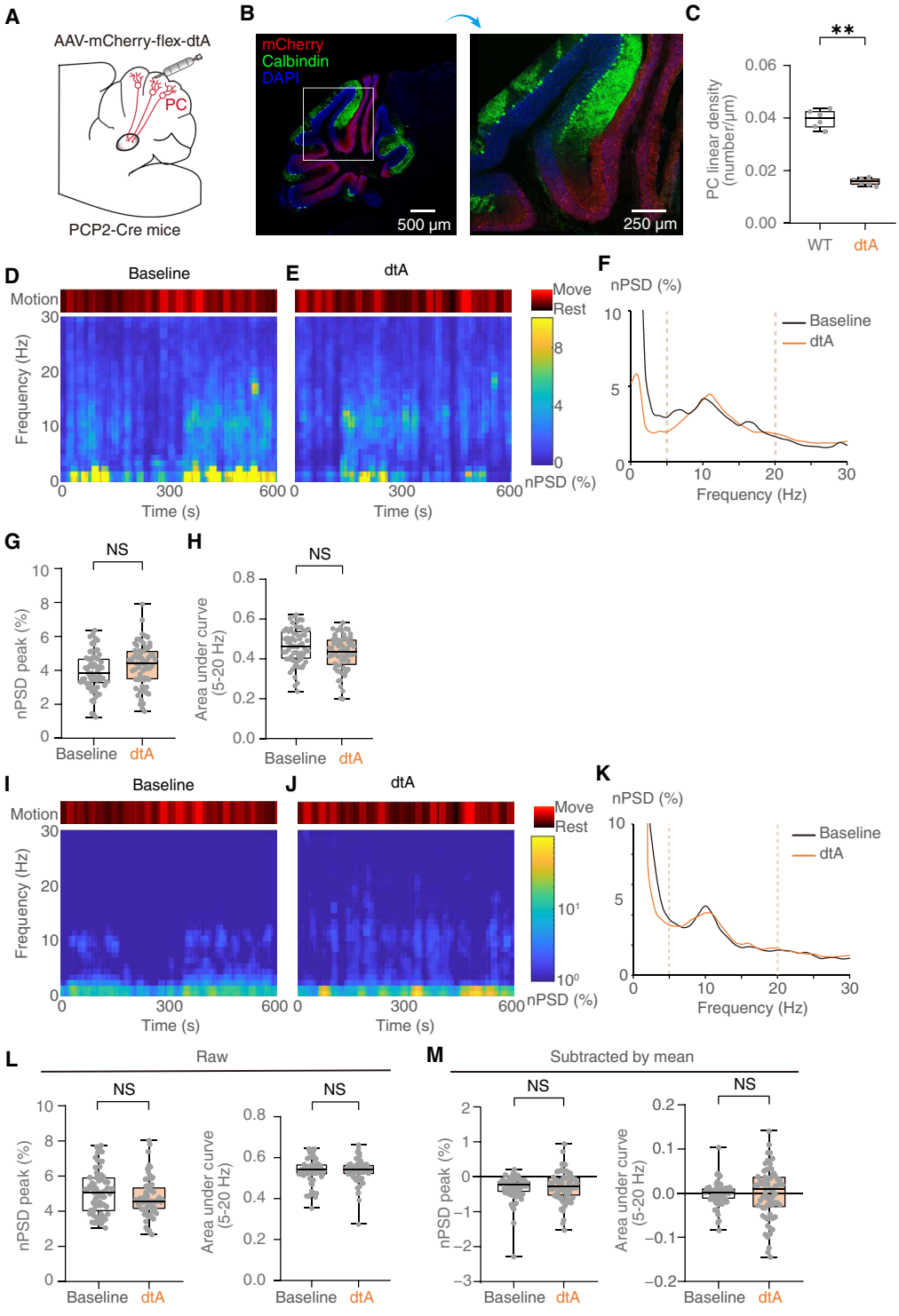

Fig. 4. Lesioning of PCs does not affect motor and cerebellar rhythms in mice. (**A**) Schematic illustration of AAV9-mCherry-flex-dtA injection into the cerebellar cortex in *PCP2-cre* mice. (**B**) Representative histology of PC-specific lesioning induced by diphtheria toxin A (dtA) expression. Alive PCs are calbindin (+), and lesioned PCs are mCherry (+). (**C**) Quantitative assessment of Purkinje cell linear density in wild-type control versus PC-lesioned mice ($n = 6$ mice in each group). (**D** to **F**) Representative time-frequency plots of recorded motor rhythms [(D) and (E)] and corresponding normalized spectral diagrams, nPSDs (F) of mice before and after virus-driven PC lesioning by diphtheria toxin. (**G** and **H**) Group analysis ($n = 6$ mice, 11 sections of each mouse to match the length of stGtACR2 timeframes for comparison). NS, not significant. (**I** to **K**) Representative time-frequency plots [(I) and (J)] and nPSDs (K). (**L** and **M**) Group analysis ($n = 6$ mice, 11 sections of each mouse). Data are presented with box and whisker plots. $^{**}P < 0.01$, Mann-Whitney *U* tests.

showed reduced cerebellar oscillatory patterns toward the 1/*f* background (Fig. 5, E to G).

Cerebellar rhythm loss is a shared feature observed in cerebellar ataxia of various causes

Although the data from patients with IO damage provided valuable information, pure IO degeneration is extremely rare and unlikely to be systemically studied. Given that we observed CF synaptic loss in different causes of cerebellar ataxia (Fig. 1, A to J), we next asked whether loss of cerebellar rhythm could be a shared electrophysiological signature in patients with various causes of cerebellar ataxia. Cerebellar EEG was recorded from healthy volunteers and patients with cerebellar ataxia with diverse genetic and nongenetic causes (Fig. 6, A to C; demographics in table S3). We observed a reduction in cerebellar rhythm (Fig. 6C) and a significant reduction in normalized PSDs (Fig. 6D, gray-shaded window: 4 to 15 Hz, $P < 0.05$) in patients with ataxia as compared with healthy controls. We then measured the cerebellar rhythm index (CRI) by detecting the regional minimum of normalized PSD (see Materials and Methods). We found that the CRI was significantly lower in patients with cerebellar ataxia compared with control participants (Fig. 6E, control versus cerebellar ataxia: 1.35 ± 0.79 versus 0.84 ± 0.53, $P < 0.05$), indicating a reduction (or loss) in cerebellar rhythm. We next validated the cerebellar oscillatory features with patients with essential tremor as a positive control group known to have increased cerebellar oscillations (fig. S14, A to C) (*7*, *8*, *27*). CRI, which is designed to detect a regional minimum of PSD patterns, reliably detected cerebellar rhythm loss in patients with ataxia. On the other hand, the cerebellar oscillatory index (COI), which is designed to detect regional oscillatory peaks, reliably contrasted tremor groups from the other two groups.

We next investigated whether cerebellar rhythm loss is a general phenomenon across various causes of cerebellar ataxia. Patients diagnosed with SCA or non-SCA showed a similar degree of cerebellar rhythm loss (Fig. 6F). Such a reduction can be seen in patients with SCA, MSA-C, and ILOCA (idiopathic late-onset cerebellar ataxia) (fig. S15, A to C). These data suggested that loss of cerebellar rhythm is a common physiological change in cerebellar ataxia.

Loss of cerebellar rhythm correlates with clinic ataxia severity

We next asked whether CRI reflects clinical severity by examining the relationship between the CRI and disease severity rated by the Scale for the Assessment and Rating of Ataxia (SARA) scores. We found that the CRI negatively correlated with the clinical severity of ataxia measured by the SARA scale [Fig. 6G, correlation coefficient $(r) = -0.514$, $P = 0.021$]. The correlation was mainly driven by the axial components (Fig. 6H, $r = -0.587$, $P = 0.006$) but not the appendicular assessments of the SARA scale (Fig. 6I, $r = -0.217$, $P = 0.359$). In addition, the CRI did not correlate with disease duration (fig. S16A, $r = 0.234$, $P = 0.322$) or age of onset (fig. S16B, $r = -0.203$, $P = 0.390$). These data further support that cerebellar rhythm loss directly reflects the underlying cerebellar circuit dysfunction and clinical severity.

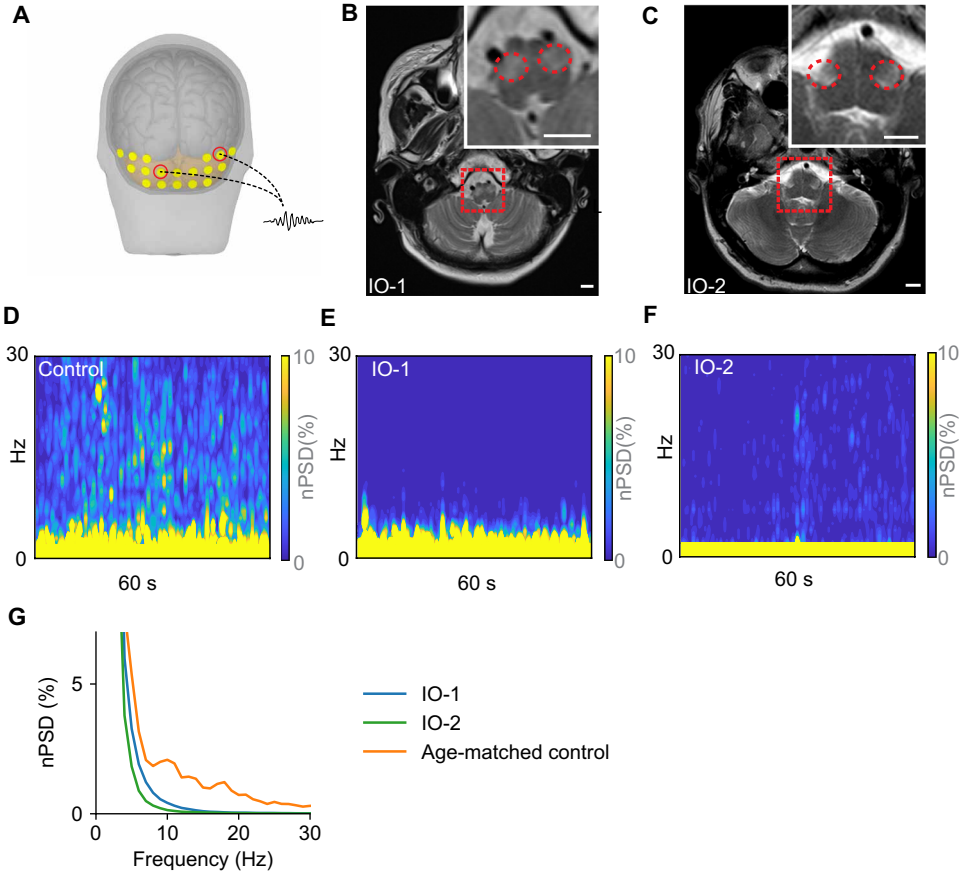

Fig. 5. Reduced cerebellar rhythms in EEG of patients with IO degeneration. (**A**) Illustration of the locations of sub-inion electrodes (yellow dots) and applied bipolar electrodes (red circles) for cerebellar EEG. (**B** and **C**) T2-weight brain MRI images from two patients with IO degeneration (IO-1 and IO-2). The insets demonstrated T2 hyperintensity in IOs, consistent with hypertrophic degeneration. IOs are circled in the insets. Scale bars, 1 cm. (**D** to **F**) Normalized spectrograms of the cerebellar EEG recordings from an age-matched control participant (D) and two patients, IO-1 (E) and IO-2 (F). (**G**) nPSDs of cerebellar EEG recordings of all three individuals [(D) to (F)].

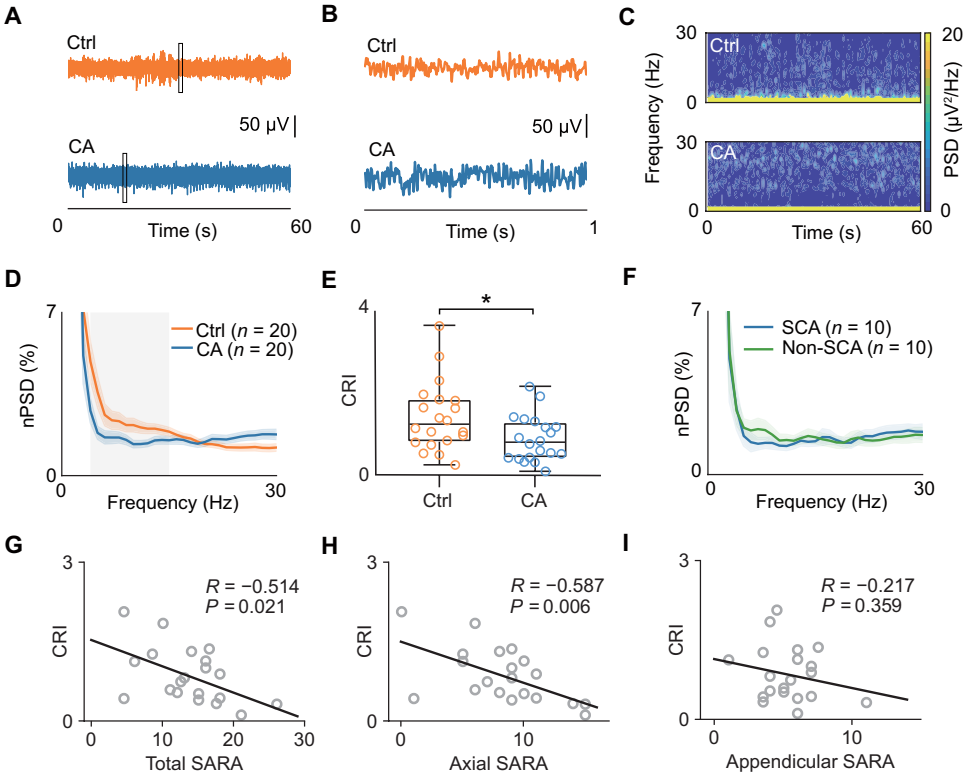

Fig. 6. Cerebellar EEG features in patients with cerebellar ataxia. (**A** and **B**) Representative 60-s raw traces (A) and zoomed 1-s segments (B) of bipolar EEG recordings from a healthy control (Ctrl) and a patient with cerebellar ataxia (CA). (**C**) Spectrogram calculated from the corresponding raw traces in (B). (**D**) Average nPSDs from control participants and patients with cerebellar ataxia ($n = 20$ for both groups). The shaded colors marked the range of SEM. The gray-shaded window encompasses the frequency band where the PSD at each frequency was statistically significantly lower in patients with CA ($P < 0.05$). (**E**) CRI in CA and Ctrl. (**F**) Average nPSDs derived from EEG recordings of patients with SCA and non-SCA patients ($n = 10$ for each group). (**G** to **I**) Correlation between SARA scores and CRIs, including total scores (G), axial subscores (H), and appendicular subscores (I) [the same 20 patients in (E)]. Data are presented with box and whisker plots. *$P < 0.05$, Mann-Whitney *U* test (E), and linear regression [(G) to (I)].

In summary, cerebellar rhythm loss is a shared electrophysiological feature in patients with various causes. The rhythm loss is not driven by causes, disease onset, or disease duration but a neurophysiological reflection directly linked to disease severity.

Chemogenetic IO stimulation shows therapeutic effects in mice

To explore whether modulation of CF activity could potentially ameliorate cerebellar ataxia, we injected a lentiviral vector with the sequence of an activating designer receptor [hM3D(Gq)] under an IO-specific promoter Htr5b(3.7) (*28*) into the IOs of SCA1 mice (fig. S17A). Intraperitoneal injection of clozapine *N*-oxide (CNO) to chemogenetically activate the IO improved the motor performance in the balance beam test (fig. S17B) and shifted the peak motor rhythm toward 10 Hz (fig. S17, C to F). Video-based gait analysis did not reveal significant gait deficits in SCA1 mice ($P > 0.05$), with or without CNO administration (fig. S18, A to E). Chemogenetic activation of CF activity improved cerebellar and motor rhythm as well as some metrics of motor performance in ataxic mice.

DISCUSSION

In this study, we identified CF synaptic loss as a common pathological feature and reduced cerebellar rhythm as a common physiological attribute in patients with cerebellar ataxia. We found that patients with different causes of cerebellar ataxia developed cerebellar rhythm loss, which correlated with clinical severity. Optogenetic suppression of CF synaptic activity in mice reduced cerebellar rhythm and triggered ataxia-like behaviors including motor rhythm loss and impaired motor precision. Chemogenetic activation of CF improved both motor rhythm and precision in a SCA1 mouse model. Collectively, our study established a framework for common circuit changes in cerebellar ataxia and suggests CF as a therapeutic target for cerebellar ataxia. The results are summarized in fig. S19.

One of our key findings is that reduced cerebellar rhythm correlates with ataxia severity (Fig. 6) but not with causes, age of onset, or disease duration. This suggests that the cerebellar rhythm reflects the circuit integrity of cerebellar ataxia. Although it is still unclear how loss of cerebellar rhythm progresses over time in patients, this measurement may have the potential to track disease progression. Incorporating such an objective parameter will be crucial in clinical trials developing therapies for cerebellar ataxia. Of note, cerebellar oscillations can be altered in other diseases, such as essential tremor (*7*, *8*, *27*, *29*) and Parkinson's disease (*30*–*32*). The measurement of cerebellar rhythm reduction should be applied for evaluating patients with a confirmed diagnosis of cerebellar ataxia but not used as a biomarker for differential diagnosis.

Several recent studies have shown that frequency-dependent stimulations to the deep cerebellar nuclei (DCN) can improve motor function in rodent models of cerebellar ataxia (*33*, *34*). For example, Anderson *et al.* showed that stimulating the dorsal dentate nucleus at 30 Hz effectively reduced motor symptoms in *Shaker* rats (*33*). Miterko *et al.* demonstrated that beta-frequency stimulation at the interposed nucleus improved motor behavior in *Car8* mice (*34*). Although the stimulations in these studies were not directly targeted to the CFs, DCN is the major final output of the cerebellum; therefore, stimulation at DCN, which is downstream of CF synapses, likely overrides the aberrant activities originating from the cerebellar cortex, achieving a therapeutic effect. Consistent with the idea of

normalizing cerebellar physiology, noninvasive neuromodulation, such as transcranial direct current stimulation, has been shown to improve cerebellar ataxia (*35*–*40*). Cerebellar EEG technique and monitoring cerebellar rhythm are likely to guide the creation of more effective stimulation paradigms and allow a close-loop stimulation design.

CFs form thousands of synaptic contacts with each PC, facilitating reliable signal transmission from IO neurons (*41*). IO neurons have intrinsic oscillatory properties (*42*, *43*) and achieve interneuronal synchrony by direct electrical coupling through gap junctions (*44*, *45*). These characteristics may be crucial for generating the cerebellar oscillations necessary for coordinating daily movements, providing a potential explanation for the severe ataxia and rhythm disturbances observed in this study when IO activity is disrupted. In SCA1[82Q] mice, there is a marked reduction in PC responses to CF activation (*4*). Direct lesioning or silencing of IO can cause various motor deficits in cats (*46*, *47*). Conversely, excessive IO-to-PC synchrony due to CF overgrowth can lead to an abnormal amplification of cerebellar rhythms, resulting in conditions such as essential tremor (*7*, *8*, *48*). When CF-to-PC activity is normal, lesioning up to 60% of PCs in WT mice did not cause cerebellar or motor rhythm deficits (Fig. 5, A to O), suggesting a strong reserve of PCs for motor rhythm generation. When CF-to-PC activity is reduced (in ataxia) or excessive (in tremors), the cerebellum generates abnormal rhythms that directly affect motor rhythms and cause coordination deficits.

This study has limitations. Because of the small sample size for each type of patient with cerebellar ataxia, further studies of larger sample sizes in different types of cerebellar ataxia are needed to clarify the detailed relationship between loss of cerebellar rhythm and individual causes of cerebellar ataxia. However, the loss of cerebellar rhythm appears to be a shared physiological feature across the various causes of cerebellar ataxia tested, indicating a common circuit mechanism. In the mouse investigations, we did not address the laterality issue of IO-to-PC transmissions. IO is a midline structure, and illuminating the highly sensitive stGtACR2 from either side prompts inhibition of bilateral IOs. Cranial window–based miniSOG activation can affect widespread CF synapses, with a drawback of suboptimal focality. Further studies are required to unravel the laterality effect. We did not record single-unit activities during optogenetic manipulations. How the neuronal activity changes lead to cerebellar local field changes requires further investigation. We did not collect simultaneous single-unit activities of the IOs in CF-silencing mice or SCA1 mice. Further studies are required to understand IO neuronal firings and the spatiotemporal assembly of populational neuronal activities, which may be different in each goal-directed movement. The information is critical to optimizing CF-related therapy in a motion-specific manner.

In conclusion, CF synaptic loss contributes to cerebellar ataxia symptoms and thus may be considered a therapeutic target. Whether loss of cerebellar rhythm, a shared physiological feature, could be used as a marker to monitor the cerebellar circuit responses to therapies warrants further studies. The presented findings will allow us to support the design of future synaptic intervention trials for cerebellar ataxia.

MATERIALS AND METHODS

Study design

This study investigated CF pathophysiology and its contributions to ataxic symptoms across mice and patients with various etiologies. In vivo electrophysiological recordings, combined with optogenetic or chemogenetic manipulations, were conducted in WT and SCA1[82Q] ataxic mice. The mice performed tasks such as balance-beam walking, video-based gait analysis, or force plate motor rhythm tracking. To manipulate CF-to-PC activity and assess its contribution to cerebellar rhythm alterations and ataxic behaviors, optogenetic silencing of IO or CF synapses was applied using virally transfected tools. Chemogenetic activation of IO neurons was performed in SCA1 mice as a proof of concept to improve ataxia-related motor rhythms and motor performance. All experiments in mice adhered to the Animal Research: Reporting of In Vivo Experiments (ARRIVE) guidelines and were approved by the Institutional Animal Care and Use Committee in Columbia University (no. AABI3610) and National Taiwan University (no. B202000003). Cerebellar EEG recordings were also obtained from healthy individuals and patients diagnosed with SCA1, SCA2, SCA6, dentatorubral-pallidoluysian atrophy (DRPLA), MSA-C, or IO degeneration. We examined the loss of cerebellar rhythms and their correlation with clinical ataxia severity, measured by the SARA score. All experimental protocols and sample sizes in both mice and human studies were reviewed and approved by ethical committees on the basis of power analysis. The human-arm investigation followed the Strengthening the Reporting of Observational Studies in Epidemiology (STROBE) guidelines of cross-sectional studies. All the clinical procedures were approved by the institutional review board at Columbia University (no. AAAU0162) and National Taiwan University Hospital (no. 201801032RINB). All participants signed the informed consent approved by the Institutional Review Board of Columbia University or National Taiwan University Hospital. All animal and human trials, except for chemogenetic experiments, were analyzed in a single-blind design, where the evaluators were unaware of the experimental manipulations or patient diagnoses. Optogenetic manipulations were self-controlled within a single session without randomization. Chemogenetic manipulations, involving CNO or saline controls, were double blinded with randomized administration. All experimental mice had proper signal qualities (for electrophysiology) and expression of viral constructs (for optogenetics and chemogenetics), and we included all data points. We also included all data points of human participants.

Statistical analysis

Statistical analyses were performed with the SciPy package from Python or with Matlab. Descriptive data are presented as means ± SEM. Each variable was tested for normal distribution using Kolmogorov-Smirnov tests. For two-group comparisons, Student's *t* tests were used to compare the normally distributed variables. Mann-Whitney *U* tests and Wilcoxon signed-rank tests were used to compare the variables that are not normally distributed. Spearman's correlation analyses were used to test the correlation between nonparametric variables. Two-tailed *P* values of less than 0.05 were considered statistically significant. Effect size was calculated by the Matlab "meanEffectSize" function.

Supplementary Materials

The PDF file includes:

Materials and Methods
Figs. S1 to S19
Tables S1 to S3
Legends for movies S1 to S5
References (*49*–*59*)

Other Supplementary Material for this manuscript includes the following:
Movies S1 to S5
Data file S1
MDAR Reproducibility Checklist

REFERENCES AND NOTES

1. C. R. Lin, S. H. Kuo, Ataxias: Hereditary, acquired, and reversible etiologies. *Semin. Neurol.* **43**, 48–64 (2023).
2. S. H. Kuo, Ataxia. *Continuum* **25**, 1036–1054 (2019).
3. K. T. Kwei, S. H. Kuo, An overview of the current state and the future of ataxia treatments. *Neurol. Clin.* **38**, 449–467 (2020).
4. J. A. Barnes, B. A. Ebner, L. A. Duvick, W. Gao, G. Chen, H. T. Orr, T. J. Ebner, Abnormalities in the climbing fiber-Purkinje cell circuitry contribute to neuronal dysfunction in *ATXN1[82Q]* mice. *J. Neurosci.* **31**, 12778–12789 (2011).
5. B. A. Ebner, M. A. Ingram, J. A. Barnes, L. A. Duvick, J. L. Frisch, H. B. Clark, H. Y. Zoghbi, T. J. Ebner, H. T. Orr, Purkinje cell ataxin-1 modulates climbing fiber synaptic input in developing and adult mouse cerebellum. *J. Neurosci.* **33**, 5806–5820 (2013).
6. S. A. Furrer, S. M. Waldherr, M. S. Mohanachandran, T. D. Baughn, K. T. Nguyen, B. L. Sopher, V. A. Damian, G. A. Garden, A. R. La Spada, Reduction of mutant ataxin-7 expression restores motor function and prevents cerebellar synaptic reorganization in a conditional mouse model of SCA7. *Hum. Mol. Genet.* **22**, 890–903 (2013).
7. Y. M. Wang, C. W. Liu, S. Y. Chen, L. Y. Lu, W. C. Liu, J. H. Wang, C. L. Ni, S. B. Wong, A. Kumar, J. C. Lee, S. H. Kuo, S. C. Wu, M. K. Pan, Neuronal population activity in the olivocerebellum encodes the frequency of essential tremor in mice and patients. *Sci. Transl. Med.* **16**, eadl1408 (2024).
8. M. K. Pan, Y. S. Li, S. B. Wong, C. L. Ni, Y. M. Wang, W. C. Liu, L. Y. Lu, J. C. Lee, E. P. Cortes, J. G. Vonsattel, Q. Sun, E. D. Louis, P. L. Faust, S. H. Kuo, Cerebellar oscillations driven by synaptic pruning deficits of cerebellar climbing fibers contribute to tremor pathophysiology. *Sci. Transl. Med.* **12**, eaay1769 (2020).
9. S. L. Palay, V. Chan-Palay, *Cerebellar Cortex: Cytology and Organization* (Springer Science & Business Media, 2012).
10. M. Watanabe, Molecular mechanisms governing competitive synaptic wiring in cerebellar Purkinje cells. *Tohoku J. Exp. Med.* **214**, 175–190 (2008).
11. M. Mahn, L. Gibor, P. Patil, K. Cohen-Kashi Malina, S. Oring, Y. Printz, R. Levy, I. Lampl, O. Yizhar, High-efficiency optogenetic silencing with soma-targeted anion-conducting channelrhodopsins. *Nat. Commun.* **9**, 4125 (2018).
12. J. Y. Lin, S. B. Sann, K. Zhou, S. Nabavi, C. D. Proulx, R. Malinow, Y. Jin, R. Y. Tsien, Optogenetic inhibition of synaptic release with chromophore-assisted light inactivation (CALI). *Neuron* **79**, 241–253 (2013).
13. C. L. Ni, Y. T. Lin, L. Y. Lu, J. H. Wang, W. C. Liu, S. H. Kuo, M. K. Pan, Tracking motion kinematics and tremor with intrinsic oscillatory property of instrumental mechanics. *Bioeng. Transl. Med.* **8**, e10432 (2023).
14. A. M. Brown, J. J. White, M. E. van der Heijden, J. Zhou, T. Lin, R. V. Sillitoe, Purkinje cell misfiring generates high-amplitude action tremors that are corrected by cerebellar deep brain stimulation. *eLife* **9**, e51928 (2020).
15. H. B. Clark, E. N. Burright, W. S. Yunis, S. Larson, C. Wilcox, B. Hartman, A. Matilla, H. Y. Zoghbi, H. T. Orr, Purkinje cell expression of a mutant allele of SCA1 in transgenic mice leads to disparate effects on motor behaviors, followed by a progressive cerebellar dysfunction and histological alterations. *J. Neurosci.* **17**, 7385–7395 (1997).
16. J. J. White, L. W. J. Bosman, F. G. C. Blot, C. Osório, B. W. Kuppens, W. Krijnen, C. Andriessen, C. I. De Zeeuw, D. Jaarsma, M. Schonewille, Region-specific preservation of Purkinje cell morphology and motor behavior in the ATXN1[82Q] mouse model of spinocerebellar ataxia 1. *Brain Pathol.* **31**, e12946 (2021).
17. F. G. C. Blot, W. Krijnen, S. Den Hoedt, C. Osório, J. J. White, M. T. Mulder, M. Schonewille, Sphingolipid metabolism governs Purkinje cell patterned degeneration in *Atxn1[82Q]/+* mice. *Proc. Natl. Acad. Sci. U.S.A.* **118**, e2016969118 (2021).
18. W. Qu, A. Johnson, J. H. Kim, A. Lukowicz, D. Svedberg, M. Cvetanovic, Inhibition of colony-stimulating factor 1 receptor early in disease ameliorates motor deficits in SCA1 mice. *J. Neuroinflammation* **14**, 107 (2017).
19. M. F. Ibrahim, E. M. Power, K. Potapov, R. M. Empson, Motor and cerebellar architectural abnormalities during the early progression of ataxia in a mouse model of SCA1 and how early prevention leads to a better outcome later in life. *Front. Cell. Neurosci.* **11**, 292 (2017).
20. N. L. Cerminara, J. A. Rawson, Evidence that climbing fibers control an intrinsic spike generator in cerebellar Purkinje cells. *J. Neurosci.* **24**, 4510–4517 (2004).
21. F. Bengtsson, P. Svensson, G. Hesslow, Feedback control of Purkinje cell activity by the cerebello-olivary pathway. *Eur. J. Neurosci.* **20**, 2999–3005 (2004).
22. R. J. Barry, F. M. De Blasio, Characterizing pink and white noise in the human electroencephalogram. *J. Neural Eng.* **18**, 034001 (2021).
23. K. H. Pettersen, H. Lindén, T. Tetzlaff, G. T. Einevoll, Power laws from linear neuronal cable theory: Power spectral densities of the soma potential, soma membrane current and single-neuron contribution to the EEG. *PLOS Comput. Biol.* **10**, e1003928 (2014).
24. S. X. Moffett, S. M. O'Malley, S. Man, D. Hong, J. V. Martin, Dynamics of high frequency brain activity. *Sci. Rep.* **7**, 15758 (2017).
25. M. W. C. Rousseaux, T. Tschumperlin, H. C. Lu, E. P. Lackey, V. V. Bondar, Y. W. Wan, Q. Tan, C. J. Adamski, J. Friedrich, K. Twaroski, W. Chen, J. Tolar, C. Henzler, A. Sharma, A. Bajić, T. Lin, L. Duvick, Z. Liu, R. V. Sillitoe, H. Y. Zoghbi, H. T. Orr, ATXN1-CIC complex is the primary driver of cerebellar pathology in spinocerebellar ataxia type 1 through a gain-of-function mechanism. *Neuron* **97**, 1235–1243.e5 (2018).
26. L. Tejwani, N. G. Ravindra, C. Lee, Y. Cheng, B. Nguyen, K. Luttik, L. Ni, S. Zhang, L. M. Morrison, J. Gionco, Y. Xiang, J. Yoon, H. Ro, F. Haidery, R. M. Grijalva, E. Bae, K. Kim, R. T. Martuscello, H. T. Orr, H. Y. Zoghbi, H. S. McLoughlin, L. P. W. Ranum, V. G. Shakkottai, P. L. Faust, S. Wang, D. van Dijk, J. Lim, Longitudinal single-cell transcriptional dynamics throughout neurodegeneration in SCA1. *Neuron* **112**, 362–383.e15 (2024).
27. S. B. Wong, Y. M. Wang, C. C. Lin, S. K. Geng, N. Vanegas-Arroyave, S. L. Pullman, S. H. Kuo, M. K. Pan, Cerebellar oscillations in familial and sporadic essential tremor. *Cerebellum* **21**, 425–431 (2022).
28. K. Dorgans, D. Guo, K. Kurima, J. Wickens, M. Y. Uusisaari, Designing AAV vectors for monitoring the subtle calcium fluctuations of inferior olive network in vivo. *Front. Cell. Neurosci.* **16**, 825056 (2022).
29. A. Kumar, C. C. Lin, S. H. Kuo, M. K. Pan, Physiological recordings of the cerebellum in movement disorders. *Cerebellum* **22**, 985–1001 (2023).
30. T. J. Bosch, A. I. Espinoza, A. Singh, Cerebellar oscillatory dysfunction during lower-limb movement in Parkinson's disease with freezing of gait. *Brain Res.* **1808**, 148334 (2023).
31. T. J. Bosch, S. Kammermeier, C. Groth, M. Leedom, E. K. Hanson, P. Berg-Poppe, A. Singh, Cortical and cerebellar oscillatory responses to postural instability in Parkinson's disease. *Front. Neurol.* **12**, 752271 (2021).
32. T. J. Bosch, C. Groth, T. A. Eldridge, E. Z. Gnimpieba, L. A. Baugh, A. Singh, Altered cerebellar oscillations in Parkinson's disease patients during cognitive and motor tasks. *Neuroscience* **475**, 185–196 (2021).
33. C. J. Anderson, K. P. Figueroa, A. D. Dorval, S. M. Pulst, Deep cerebellar stimulation reduces ataxic motor symptoms in the shaker rat. *Ann. Neurol.* **85**, 681–690 (2019).
34. L. N. Miterko, T. Lin, J. Zhou, M. E. van der Heijden, J. Beckinghausen, J. J. White, R. V. Sillitoe, Neuromodulation of the cerebellum rescues movement in a mouse model of ataxia. *Nat. Commun.* **12**, 1295 (2021).
35. A. Benussi, G. Koch, M. Cotelli, A. Padovani, B. Borroni, Cerebellar transcranial direct current stimulation in patients with ataxia: A double-blind, randomized, sham-controlled study. *Mov. Disord.* **30**, 1701–1705 (2015).
36. A. Benussi, V. Dell'Era, M. S. Cotelli, M. Turla, C. Casali, A. Padovani, B. Borroni, Long term clinical and neurophysiological effects of cerebellar transcranial direct current stimulation in patients with neurodegenerative ataxia. *Brain Stimul.* **10**, 242–250 (2017).
37. A. Benussi, V. Dell'Era, V. Cantoni, E. Bonetta, R. Grasso, R. Manenti, M. Cotelli, A. Padovani, B. Borroni, Cerebello-spinal tDCS in ataxia: A randomized, double-blind, sham-controlled, crossover trial. *Neurology* **91**, e1090–e1101 (2018).
38. T. L. Barretto, I. D. Bandeira, J. G. Jagersbacher, B. L. Barretto, E. T. Å. de Oliveira, N. Peña, J. G. V. Miranda, R. Lucena, Transcranial direct current stimulation in the treatment of cerebellar ataxia: A two-phase, double-blind, auto-matched, pilot study. *Clin. Neurol. Neurosurg.* **182**, 123–129 (2019).
39. L. A. Grecco, C. S. Oliveira, N. A. Duarte, V. L. Lima, N. Zanon, F. Fregni, Cerebellar transcranial direct current stimulation in children with ataxic cerebral palsy: A sham-controlled, crossover, pilot study. *Dev. Neurorehabil.* **20**, 142–148 (2017).
40. T. X. Chen, C. Y. Yang, G. Willson, C. C. Lin, S. H. Kuo, The efficacy and safety of transcranial direct current stimulation for cerebellar ataxia: A systematic review and meta-analysis. *Cerebellum* **20**, 124–133 (2021).
41. F. Rossi, C. Saggiorato, P. Strata, Target-specific innervation of embryonic cerebellar transplants by regenerating olivocerebellar axons in the adult rat. *Exp. Neurol.* **173**, 205–212 (2002).
42. R. Llinás, Y. Yarom, Oscillatory properties of guinea-pig inferior olivary neurones and their pharmacological modulation: An in vitro study. *J. Physiol.* **376**, 163–182 (1986).
43. R. Llinas, R. A. Volkind, The olivo-cerebellar system: Functional properties as revealed by harmaline-induced tremor. *Exp. Brain Res.* **18**, 69–87 (1973).
44. E. J. Lang, I. Sugihara, R. Llinas, Olivocerebellar modulation of motor cortex ability to generate vibrissal movements in rat. *J. Physiol.* **571**, 101–120 (2006).
45. E. J. Lang, I. Sugihara, R. Llinás, GABAergic modulation of complex spike activity by the cerebellar nucleoolivary pathway in rat. *J. Neurophysiol.* **76**, 255–275 (1996).
46. K. M. Horn, M. Pong, A. R. Gibson, Functional relations of cerebellar modules of the cat. *J. Neurosci.* **30**, 9411–9423 (2010).
47. K. M. Horn, A. Deep, A. R. Gibson, Progressive limb ataxia following inferior olive lesions. *J. Physiol.* **591**, 5475–5489 (2013).

48. A. Handforth, E. J. Lang, Increased Purkinje cell complex spike and deep cerebellar nucleus synchrony as a potential basis for syndromic essential tremor. A review and synthesis of the literature. *Cerebellum* **20**, 266–281 (2021).
49. R. J. Louis, C. Y. Lin, P. L. Faust, A. H. Koeppen, S. H. Kuo, Climbing fiber synaptic changes correlate with clinical features in essential tremor. *Neurology* **84**, 2284–2286 (2015).
50. S. H. Kuo, C. Y. Lin, J. Wang, J. Y. Liou, M. K. Pan, R. J. Louis, W. P. Wu, J. Gutierrez, E. D. Louis, P. L. Faust, Deep brain stimulation and climbing fiber synaptic pathology in essential tremor. *Ann. Neurol.* **80**, 461–465 (2016).
51. M. Pool, J. Thiemann, A. Bar-Or, A. E. Fournier, NeuriteTracer: A novel ImageJ plugin for automated quantification of neurite outgrowth. *J. Neurosci. Methods* **168**, 134–139 (2008).
52. S. H. Kuo, C. Y. Lin, J. Wang, P. A. Sims, M. K. Pan, J. Y. Liou, D. Lee, W. J. Tate, G. C. Kelly, E. D. Louis, P. L. Faust, Climbing fiber-Purkinje cell synaptic pathology in tremor and cerebellar degenerative diseases. *Acta Neuropathol.* **133**, 121–138 (2017).
53. R. Babij, M. Lee, E. Cortes, J. P. Vonsattel, P. L. Faust, E. D. Louis, Purkinje cell axonal anatomy: Quantifying morphometric changes in essential tremor versus control brains. *Brain* **136**, 3051–3061 (2013).
54. E. N. Burright, H. B. Clark, A. Servadio, T. Matilla, R. M. Feddersen, W. S. Yunis, L. A. Duvick, H. Y. Zoghbi, H. T. Orr, SCA1 transgenic mice: A model for neurodegeneration caused by an expanded CAG trinucleotide repeat. *Cell* **82**, 937–948 (1995).
55. N. Horii-Hayashi, M. Nishi, Protocol for behavioral tests using chemogenetically manipulated mice. *STAR Protoc.* **2**, 100418 (2021).
56. I. Balbo, F. Montarolo, F. Genovese, F. Tempia, E. Hoxha, Effects of the administration of Elovl5-dependent fatty acids on a spino-cerebellar ataxia 38 mouse model. *Behav. Brain Funct.* **18**, 8 (2022).
57. E. Hoxha, E. Boda, F. Montarolo, R. Parolisi, F. Tempia, Excitability and synaptic alterations in the cerebellum of APP/PS1 mice. *PLOS ONE* **7**, e34726 (2012).
58. A. Mathis, P. Mamidanna, K. M. Cury, T. Abe, V. N. Murthy, M. W. Mathis, M. Bethge, DeepLabCut: Markerless pose estimation of user-defined body parts with deep learning. *Nat. Neurosci.* **21**, 1281–1289 (2018).
59. S. Gilman, G. K. Wenning, P. A. Low, D. J. Brooks, C. J. Mathias, J. Q. Trojanowski, N. W. Wood, C. Colosimo, A. Dürr, C. J. Fowler, H. Kaufmann, T. Klockgether, A. Lees, W. Poewe, N. Quinn, T. Revesz, D. Robertson, P. Sandroni, K. Seppi, M. Vidailhet, Second consensus statement on the diagnosis of multiple system atrophy. *Neurology* **71**, 670–676 (2008).

Acknowledgment: We thank the support by the Featured Areas Research Center Program within the framework of the Higher Education Sprout Project cofunded by the National Science and Technology Council (NSTC) and the Ministry of Education, Taiwan. We thank A. H. Koeppen (Veterans Affairs Medical Center, Albany, New York, USA), the NIH NeuroBiobank [including the University of Maryland Brain and Tissue Bank (Baltimore, MD, USA), University of Miami Brain Endowment Bank (Miami, FL, USA), and Harvard Brain Tissue Resource Center, McLean Hospital (Belmont, MA, USA)], the New York Brain Bank at Columbia University (New York, NY, USA), and all the patients and families for generously providing postmortem brain tissues from healthy control and patients with cerebellar ataxia. We thank the technical assistance of the First Core Labs in the National Taiwan University College of Medicine. **Funding:** This research was supported by the NSTC in Taiwan [grants 109-2326-B-002-013-MY4 (to M.-K.P.), 107-2321-B-002-020 (to M.-K.P.), 108-2321-B-002-011 (to M.-K.P.), 108-2321-002-059-MY2 (to M.-K.P.), 110-2321-B-002-012 (to M.-K.P.), 111-2628-B-002-036 (to M.-K.P.) and 113-2628-B-002-002 (to M.-K.P.)], National Health Research Institutes [grant NHRI-EX113-11303NI (to M.-K.P.)], National Taiwan University College of Medicine [grant NTUMC 110C101-011 (to M.-K.P.)], National Taiwan University Hospital [grants NSC-145-11 (to M.-K.P.), 113-UN0013, 112-UN0024 (to M.-K.P.), 113-E0001 (to M.-K.P.), and 108-039 (to M.-K.P.)], and Academia Sinica [grant AS-TM-110-01-02 (to M.-K.P.)]. This research was also funded by the National Institutes of Health (NIH) [NINDS no. R21 NS077094, NINDS no. R01 NS085136 (to P.L.F.), NINDS no. R01 NS088257 (to P.L.F.), NINDS no. R01 NS094607 (to E.D.L.), NINDS no. R01 NS085136 (to E.D.L.), NINDS no. R01 NS073872 (to E.D.L.), NINDS no. R01 NS085136 (to E.D.L.), NINDS no. R01 NS088257 (to E.D.L.), NINDS no. R01 NS104423 (to S.-H.K.), NINDS no. R03 NS114871 (to S.-H.K.), and NINDS no. R13 NS117005 (to S.-H.K.)], National Ataxia Foundation, Parkinson's Foundation (to S.-H.K.), International Essential Tremor Foundation (to S.-H.K.), Brain Research Foundation (to S.-H.K.) and Young Investigator Award from National Ataxia Foundation (to C.-C.L.). **Author contributions:** M.-K.P., K.-C.F., T.-Y.L., and W.-C.L. performed and processed mouse behavioral experiments, cerebellar electrophysiology, and cerebellar histology with or without optogenetic manipulation. K.-C.F., Y.-L.H., and K.-C.Y. performed PC-specific lesioning. I.B. performed behavioral experiments and chemogenetic manipulations in SCA1 mice. C.-C.L. and Y.-M.W. performed cerebellar electrophysiology in human participants. C.-C.L., Y.-M.W., and S.K.G. performed EEG signal processing. C.-L.N., C.P.D., D.S.R., A.M., N.A., N.D., P.L.F., E.D.L., and S.-H.K. processed human cerebellar pathology. M.-K.P., K.-C.F., T.-Y.L., C.-C.L., and W.-C.L. optimized the Matlab codes for signal processing. All authors contribute to the writing of the manuscripts. M.-K.P. and S.-H.K. performed the final editing of the manuscript. **Competing interests:** M.-K.P. and S.-H.K. are consultants for Praxis Precision Medicines (Cambridge, Massachusetts, USA) and BioPro Scientific (Taiwan). M.-K.P. is a consultant for Sumitomo Pharma Co. (Japan). M.-K.P. and S.-H.K. confirmed that this research is unrelated to the consulting roles. The other authors declare that they have no competing interests. **Data and materials availability:** All data associated with this study are present in the paper or the Supplementary Materials. Codes for mouse data analysis are deposited in Zenodo: https://doi.org/10.5281/zenodo.14732298. EEG data for patients with cerebellar ataxia and codes for analysis are deposited in Zenodo: https://doi.org/10.5281/zenodo.14737233.

Submitted 19 August 2023
Resubmitted 18 June 2024
Accepted 4 February 2025
Published 26 February 2025
10.1126/scitranslmed.adk3922